

Article

Eco-Friendly Depolymerization of Alginates by H₂O₂ and High-Frequency Ultrasonication

Yun Ha Song, Hee Chul Woo * and Jaekyoung Lee *

Department of Chemical Engineering, Pukyong National University, Busan 48547, Republic of Korea; yhsong27@pukyong.ac.kr

* Correspondence: woohc@pknu.ac.kr (H.C.W.); leejk46@pknu.ac.kr (J.L.); Tel.: +82-51-629-6433 (J.L.)

Abstract: Marine biomass has attracted attention as an environmentally sustainable energy source that can replace petroleum-based resources. Alginates, the main natural polysaccharides extracted from seaweeds, are used in various fields, such as food, pharmaceuticals, and chemical raw materials. Because the versatile applications of alginates depend on their physicochemical properties, which are controlled by their molecular weights, proper alginate depolymerization should be established. Previous approaches have limitations such as long reaction times and environmental issues. In this study, we report eco-friendly alginate depolymerization using hydrogen peroxide (H₂O₂)-induced oxidative decomposition and high-frequency ultrasonication. In oxidative decomposition, the depolymerization tendency depends on both the temperature and the use of iron oxide catalysts that can promote the Fenton reaction. Ultrasonication is effective in promoting selective depolymerization and ring-opening reactions. Oligo-alginates obtained through the precise molecular weight regulation of alginate offer potential applications in medical devices and platform chemicals.

Keywords: alginate; marine biomass; oxidative decomposition; ultrasonication; selective decomposition



Citation: Song, Y.H.; Woo, H.C.; Lee, J. Eco-Friendly Depolymerization of Alginates by H₂O₂ and High-Frequency Ultrasonication. *Clean Technol.* **2023**, *5*, 1402–1414. <https://doi.org/10.3390/cleantechnol5040069>

Academic Editors: Daniele Cespi and Dmitry Yu. Murzin

Received: 24 October 2023

Revised: 24 November 2023

Accepted: 5 December 2023

Published: 6 December 2023



Copyright: © 2023 by the authors. Licensee MDPI, Basel, Switzerland. This article is an open access article distributed under the terms and conditions of the Creative Commons Attribution (CC BY) license (<https://creativecommons.org/licenses/by/4.0/>).

1. Introduction

Various technologies have been developed to use biomass as a feedstock to produce energy sources and chemical compounds to replace current petroleum resources [1]. These technologies encompass the use of first-generation biomass, such as corn or sugarcane, for bioethanol production, as well as research on the chemical and biological conversion of second-generation biomass (lignocellulosic biomass) to obtain high-value compounds. However, first-generation biomass has the issue of increased price because it is used as a food resource [1]. Furthermore, second-generation biomass faces challenges, such as limited cultivation areas and slow growth rates, leading to socioeconomic and environmental issues in the biomass feedstock production process [1]. Conversely, third-generation biomass, such as seaweeds such as kelp and wakame, is gaining attention as a sustainable and environmentally friendly biomass source owing to its superior carbon dioxide absorption capabilities, high productivity, and the absence of a need for arable land [2]. The Republic of Korea has a good geographical and technological background for utilizing marine biomass [1]. The Republic of Korea is surrounded by sea on three sides. Furthermore, it employs competitive seaweed cultivation technology. According to the Food and Agriculture Organization (FAO) of the United Nations 2020 State of World Fisheries and Aquaculture (SOFIA 2020) report, as of 2018, the Republic of Korea's seaweed cultivation production amounted to 1,715,000 tons, ranking third among sixteen major countries. Brown algae such as *Undaria pinnatifida* and *Saccharina japonica* constitute ~68% of the total production.

Alginate is a functional hydrophilic polysaccharide primarily found in brown algae, comprising ~40% of its dry weight. As shown in Figure 1, it consists of D-mannuronic acid and L-guluronic acid units linked by 1,4-glycosidic bonds. Alginate has carboxyl (–COOH) and hydroxyl (–OH) functional groups [3,4]. Based on these characteristics, alginates

are used in various industrial applications, including in the food, pharmaceutical, and cosmetic industries [5,6]. It also serves as a raw material for bioplastics, a viscosity modifier in inks, and an eco-friendly detergent. Furthermore, it is used as a precursor for high-value platform chemicals such as furfural or furan-derived compounds [5,6]. However, the required molecular weight of alginate significantly varies across applications. To use alginates in versatile applications, it is important to control their molecular weight and establish depolymerization processes [7–10].

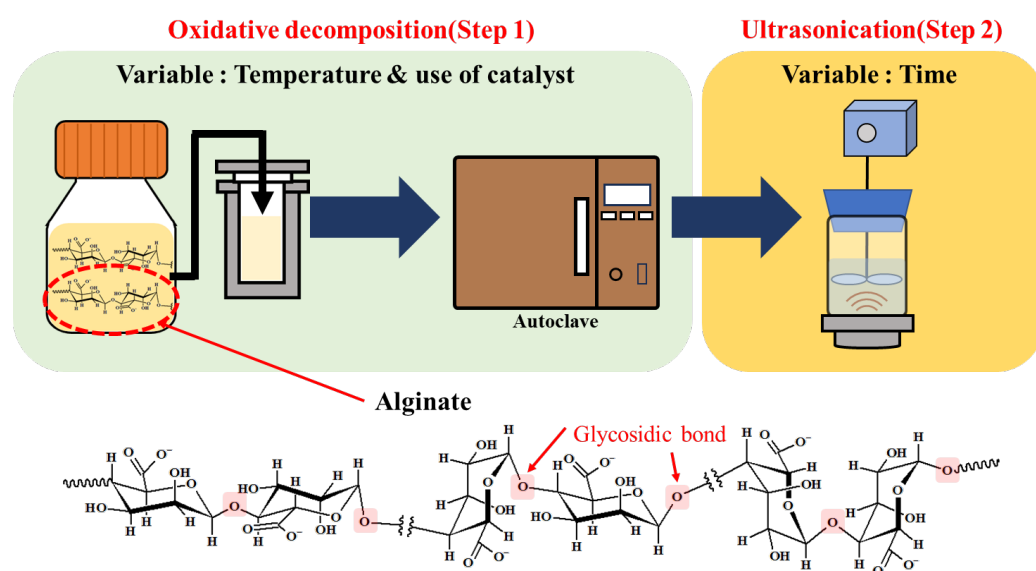


Figure 1. Schematic of alginate depolymerization.

Approaches to controlling the molecular weight of alginates can be briefly categorized into physical, biological, and chemical depolymerization [11–19]. Physical depolymerization involves microwave irradiation, ultrasonication, and thermal treatment [11–14]. Ultrasound promotes reactions through shear stress or by breaking the bonds of surrounding molecules through a cavitation effect in solution [15]. The physical approach offers the advantage of mild processing and does not require post-treatment steps, such as neutralization with low-polydispersity products. However, these methods show low reaction efficiencies and are challenging for large-scale production. Biological depolymerization uses enzymes [16,17]. While this approach exhibits high selectivity in product formation, it has the limitations of requiring post-treatment for the separation of enzymes from products and low stability owing to the biological nature of enzymes. Chemical depolymerization involves the use of acids and bases [11,15,18,19]. These methods are well suited for large-scale production. However, this method is limited by random depolymerization with diverse molecular weight distributions. Additionally, toxic chemicals require post-treatment for neutralization, leading to environmental issues. Recently, H_2O_2 , a clean chemical rather than a strong acid or base, has been used to depolymerize alginates [11,19]. Soukaina et al. reported that alginates with molecular weights of 220 kDa extracted from *Bifurcaria bifurcate* (a Moroccan brown seaweed) were depolymerized by H_2O_2 at 70 °C, leading to oligo-alginates with a molecular weight of 5.5 kDa and a degree of polymerization <24 [19]. Choi et al. reported that H_2O_2 induces the depolymerization of alginates from 450 to 15.9 kDa [11].

Despite research efforts to depolymerize alginates using physical, biological, and chemical approaches, the selective depolymerization of alginates by cleaving glycosidic linkages while preserving the monomer units of alginate has been limited. This study presents an eco-friendly depolymerization of high-molecular-weight alginates to selectively cleave glycosidic linkages within alginates via two depolymerization steps: oxidative decomposition followed by ultrasonication (Figure 1). In the first step used, hydrogen

peroxide (H_2O_2) was used as a clean oxidizing agent, facilitated by iron oxide (Fe_3O_4) catalysts to induce the Fenton reaction [20]. The second step employed high-frequency ultrasonication (~ 500 kHz) to generate hydroxyl radicals, leading to chemical effects rather than the physical effects of conventional low-frequency irradiation [15,21,22]. This approach offers a way to control the molecular weight of alginate while maintaining its inherent physicochemical properties (monomer units), thus providing oligo-alginates with molecular weights suitable for various industries.

2. Materials and Methods

2.1. Chemical Materials

Sodium alginate (Alg, 80–120 cP), purchased from Wako, Japan, was used as the raw material in this study. Hydrogen peroxide (H_2O_2 , 30 wt%) was obtained from Daejung Chemicals, Siheung, Republic of Korea and Metals Co., Ltd., Seoul, Republic of Korea. Iron (II, III) oxide, also known as black iron oxide (Fe_3O_4 , 95.0%, Samchun Chemicals, Seoul, Republic of Korea), was used as the catalyst.

2.2. Oxidative Decomposition by H_2O_2 (Step 1)

In the first step, the oxidative decomposition of alginate was performed in a batch system using an R-8 autoclave manufactured by Daeil Engineering, Seoul, Republic of Korea. Initially, a raw alginate solution was prepared by dissolving alginate in distilled water at a concentration of 2 wt%. A 2 wt% alginate solution was selected because it was appropriate to handle the solution. If the concentration increases, the solution becomes more viscous, making processing of the liquid difficult and inhomogeneous. The solution was then introduced into the reactor. Subsequently, hydrogen peroxide (H_2O_2) was added at a ratio of 1.5:1 (*w/w*) with respect to alginate, and depending on the presence or absence of the catalyst, an iron oxide catalyst (iron oxide catalyst: $\text{H}_2\text{O}_2 = 1:125$ (*w/w*)) was added. The ratio of H_2O_2 to alginate (1.5:1 *w/w*) was chosen based on previous studies [11,19]. The ratio of Fe_3O_4 to H_2O_2 was fixed at 1:125 (*w/w*) based on a previous study which reported that a similar ratio of $\text{Fe}_3\text{O}_4:\text{H}_2\text{O}_2$ was most effective during p-nitrophenol degradation by Fenton reactions with $\text{Fe}_3\text{O}_4 + \text{H}_2\text{O}_2$ [23]. Oxidative decomposition was performed at 70, 90, 110, and 130 °C for 10 h. The products obtained from the oxidative decomposition are labeled and summarized in Table 1.

Table 1. List of sample labels for oxidative decomposition.

Reaction Temperature (°C)	Use of Fe_3O_4 Catalyst	Product Label
70	No	70
90	No	90
110	No	110
130	No	130
70	Yes	F70
90	Yes	F90
110	Yes	F110
130	Yes	F130

2.3. High-Frequency Ultrasonication (Step 2)

Depolymerization through ultrasonication was conducted using a high-frequency ultrasonic device (500 kHz, 30 W) from Mirae Ultrasonic Tech. Co., Bucheon, Republic of Korea, in which 80 mL of the product obtained in Step 1 was introduced into the reactor, with the mixture then subjected to ultrasonication at 70 °C with stirring for 3, 6, and 10 h. The products obtained after ultrasonication are labeled and summarized in Table 2.

Table 2. List of sample labels for ultrasonication.

Reaction Temperature (°C)	Duration of Ultrasonication (h)	Product Label
70	3	70-U3
	6	70-U6
	10	70-U10
90	3	90-U3
	6	90-U6
	10	90-U10
110	3	110-U3
	6	110-U6
	10	110-U10
130	3	130-U3
	6	130-U6
	10	130-U10
F70	3	F70-U3
	6	F70-U6
	10	F70-U10
F90	3	F90-U3
	6	F90-U6
	10	F90-U10
F110	3	F110-U3
	6	F110-U6
	10	F110-U10
F130	3	F130-U3
	6	F130-U6
	10	F130-U10

2.4. Product Characterizations

Gel Permeation Chromatography (GPC) was used to determine the molecular weight of the products obtained after each step. The analytical columns used were a series of connected Waters Ultrahydrogel 120, 500, and 1000 columns. The mobile phase solvent used was a 0.1 M NaN₃ solution, and it was eluted at a flow rate of 1 mL/min at 40 °C.

Fourier-transform infrared (FT–IR) spectroscopy was employed to investigate the chemical and structural changes in the products obtained at each step. The FT–IR spectra were acquired using the Attenuated Total Reflection (ATR) method, and the measurements were conducted at a resolution of 4 cm^{−1} and a scanning speed of 2 mm/s.

To understand the impact of depolymerization by oxidative decomposition and ultrasonication on the molecular structure of alginate, hydrogen nuclear magnetic resonance (¹H-NMR) spectroscopy was conducted. For analysis, the products from each reaction (30 mL) were concentrated in a rotary evaporator at 35 °C. The resulting samples were dissolved in 0.75 mL of deuterated water (D₂O, 99.96% D) for analysis.

3. Results and Discussion

3.1. Oxidative Decomposition (Step 1)

3.1.1. GPC Analysis

Figures 2 and S1 and Table S1 present the results of the GPC analysis of the 2 wt% alginate used as the raw material and the products obtained from oxidative decomposition. The alginate solution had a molecular weight of ~906,000 Da and a dispersity of 4.8. When the alginate was decomposed by hydrogen peroxide (H₂O₂), the products at reaction temperatures of 70 and 90 °C showed molecular weights of ~4230 and 2380 Da, respectively, while the products at reaction temperatures of 110 and 130 °C exhibited nearly constant molecular weights at ~800 Da. Furthermore, it was observed that the dispersity of the products significantly decreased to a range of 1.36–1.58 for all reaction temperatures. This result indicates that the oxidative decomposition by H₂O₂ depolymerizes alginates into more homogeneous oligo-alginates with narrower molecular weight distributions.

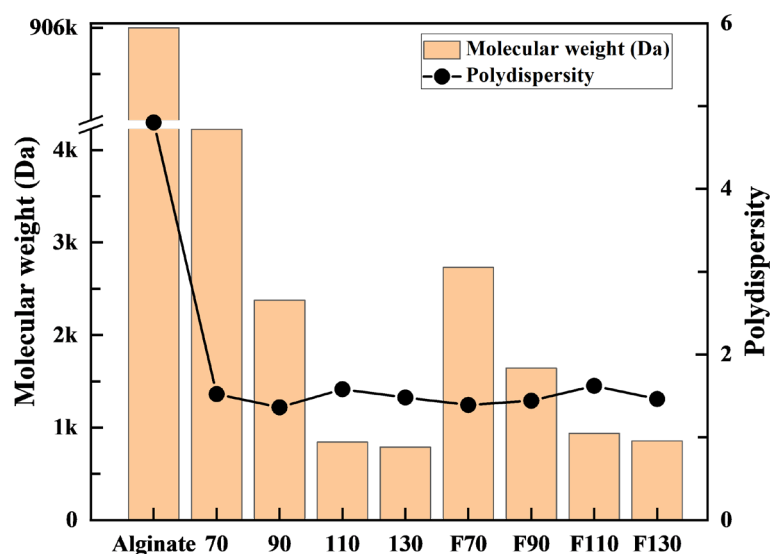


Figure 2. Molecular weight and polydispersity of alginate and products after oxidative decomposition by H_2O_2 or $\text{H}_2\text{O}_2 + \text{Fe}_3\text{O}_4$.

When using H_2O_2 and Fe_3O_4 , the products obtained at 70 and 90 °C had molecular weights of ~2730 and 1640 Da, respectively. The products obtained at reaction temperatures of 110 and 130 °C exhibited molecular weights of ~900 Da. The dispersity of all the products investigated decreased significantly to a range of 1.39–1.62. This result also shows that the oxidative decomposition by H_2O_2 and Fe_3O_4 leads to the depolymerization of alginates into more homogeneous oligo-alginates with narrower molecular weight distributions. However, no additional contribution was observed to the polydispersity of Fe_3O_4 compared with H_2O_2 alone.

From the GPC results, the products obtained at all reaction temperatures exhibited a significant decrease in molecular weight of ~99% compared with that of the raw material. However, at reaction temperatures of 70 °C and 90 °C, the Fenton reaction induced by both H_2O_2 and Fe_3O_4 occurred, increasing the generation rate of hydroxyl radicals ($\bullet\text{OH}$) and enhancing the oxidative decomposition of alginate. However, at reaction temperatures of 110 and 130 °C, the influence of Fe_3O_4 was not evident.

3.1.2. FT–IR Analysis

Figure 3a shows the FT–IR spectra of pure alginate. The spectrum reveals two groups of vibrational peaks. One is attributed to the functional groups of the alginate monomer units, namely mannuronic acid and guluronic acid, which include carboxyl anions (COO^- , 1594 cm^{-1} , 1408 cm^{-1}), pyranose ring components (1125 cm^{-1} for O–C–H, 1080 and 1045 cm^{-1} for C–O), and uronic acid residues (C–O, 950 cm^{-1}). The other group includes 1,4-glycosidic linkages (C–O–C, 1171 cm^{-1}) that connect the monomers of the alginates. These results were consistent with those of previous studies [24].

Figure 3a shows the FT–IR spectra of the oxidative decomposition products obtained using alginate and H_2O_2 alone. The peak assignments are summarized in Table S2. When the oxidative decomposition was performed at 70 and 90 °C, the peaks at 1125 and 1079 – 1081 cm^{-1} (corresponding to the pyranose ring) remained, while the peak at 1170 cm^{-1} , attributed to glycosidic linkages (C–O–C), notably decreased. From these results, it can be inferred that the applied reaction conditions did not alter the constituent units of alginate in the products but selectively cleaved the 1,4-glycosidic linkages connecting the monomers of alginate.

In the products at reaction temperatures of 110 and 130 °C, the pyranose ring-related peaks at 1125 and 1080 cm^{-1} were scarcely discernible. Moreover, strong peaks at 831 cm^{-1} (C–H bending) and 1450 cm^{-1} ($-\text{CH}_3$ and $-\text{CH}_2-$ groups) were noted [25–37]. This result indicated that ring-opening reactions occurred during oxidative decomposition.

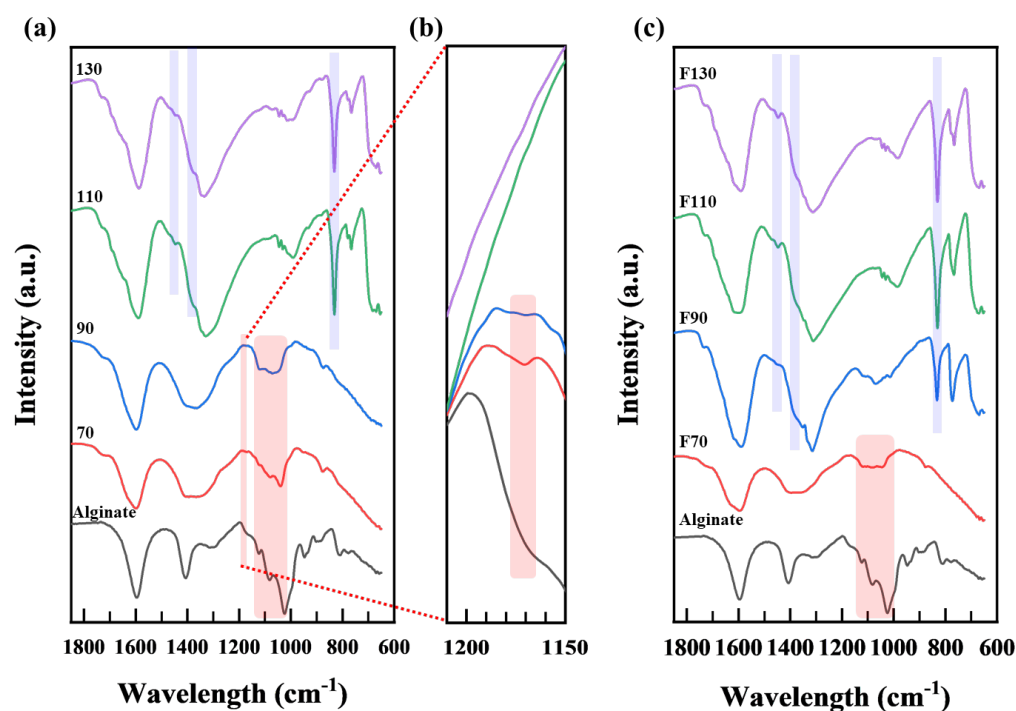


Figure 3. FT–IR spectra of products after oxidative decomposition with (a) H_2O_2 , (b) H_2O_2 ($1150\text{--}1200\text{ cm}^{-1}$), and (c) H_2O_2 and Fe_3O_4 .

Figure 3c shows the FT–IR spectra of the oxidative decomposition products obtained using alginate, H_2O_2 , and Fe_3O_4 . At a reaction temperature of $70\text{ }^\circ\text{C}$, characteristic peaks of the pyranose ring were observed at 1125 and 1081 cm^{-1} . However, vibrational peaks at 1350 cm^{-1} , attributed to the deformation vibrations of $-\text{CH}_2-$ and $-\text{CH}_3$ groups, were observed. These results suggested the presence of alginate monomer units and concurrent ring-opening reactions. Compared to alginate decomposed by only H_2O_2 at $70\text{ }^\circ\text{C}$, Fe_3O_4 catalysts result in the ring opening of alginates. By contrast, for the products obtained at reaction temperatures of $90\text{ }^\circ\text{C}$ and higher, the absorption wavelengths at 1125 and 1080 cm^{-1} , corresponding to the pyranose ring, were hardly discernible. In addition, peaks were observed at 831 cm^{-1} (C–H bending vibrations) and 1450 cm^{-1} ($-\text{CH}_3$ and $-\text{CH}_2-$ groups). This result indicates that not only were the 1,4-glycosidic linkages cleaved by the excess hydroxyl radicals ($\bullet\text{OH}$) generated from hydrogen peroxide, but also that the internal bonds within the pyranose ring were broken, forming $-\text{CH}_3$ and $-\text{CH}_2-$ groups at the terminal positions [25–37].

3.1.3. NMR Analysis

Figure 4 shows the NMR spectra of alginate and its products after oxidative decomposition. Upon examining the NMR results of pure alginate, the characteristic chemical shifts (δ) of alginate can be observed in the range of $3.5\text{--}5.6\text{ ppm}$. This observation is consistent with previous studies [38–40].

In the reaction where only H_2O_2 was used (Figure 4a), it was observed that when the reaction temperature was $<90\text{ }^\circ\text{C}$, the major peaks of alginate ($3.5\text{--}5.6\text{ ppm}$) were present. Under these conditions, only the cleavage of the glycosidic linkages occurred. Conversely, in the products obtained at reaction temperatures of 110 and $130\text{ }^\circ\text{C}$, new peaks appeared at $8.7\text{--}8.8\text{ ppm}$, corresponding to aldehyde ($-\text{CHO}$), and at $2.1\text{--}2.3\text{ ppm}$, representing methyl groups ($-\text{CH}_3$) and carbon chains ($-\text{CH}_2-$). This result indicated that the C2–C3 bond within the pyranose ring was broken during oxidative decomposition, forming aldehydes at the chain terminus. In addition, the presence of $-\text{CH}_3$ and $-\text{CH}_2-$ in the alginate backbone was suggested. These results are consistent with the degradation products of other sugars, such

as hyaluronic acid, and confirm similar outcomes for the breakdown of pyranose structures within alginate [11,38–41].

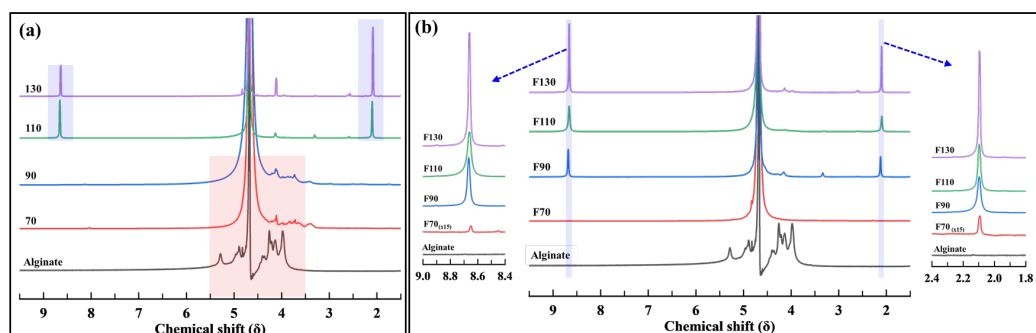


Figure 4. $^1\text{H-NMR}$ spectra of products after oxidative decomposition with (a) H_2O_2 and (b) H_2O_2 and Fe_3O_4 .

When H_2O_2 and Fe_3O_4 were used (Figure 4b), it was observed that new peaks appeared at 8.7–8.8 ppm and 2.1–2.3 ppm under all given oxidative decomposition conditions. However, at a reaction temperature of 70 °C, the characteristic chemical shifts of alginate (3.5–5.6 ppm) were also present, suggesting that glycosidic linkage cleavage and ring-opening reactions occurred simultaneously in this case [11,38–41].

In summary, reaction temperature plays a significant role in the first step of depolymerization (oxidative decomposition). Based on the GPC results, the minimum molecular weight achievable was ~800 Da, and higher reaction temperatures promoted more efficient depolymerization reactions. Furthermore, based on the FT-IR and NMR results, when only H_2O_2 was used, it is inferred that alginate monomer units were well preserved at 70 and 90 °C and that only glycosidic linkages connecting monomers were selectively cleaved. However, at the reaction temperatures of 110 and 130 °C, ring-opening reactions in alginate monomer units occurred, leading to random scission of the bonds that constitute the polymer. In the reactions using H_2O_2 and Fe_3O_4 , random scission of the alginate chains was initiated at all the reaction temperatures.

3.2. High-Frequency Ultrasonication (Step 2)

High-frequency ultrasonication was performed using alginate products depolymerized via oxidative decomposition (Step 1) as the starting material. The nomenclature of the raw materials and products used in Step 2 is summarized in Table 2.

3.2.1. GPC Analysis

Figure 5a,b and Tables S3 and S4 show the molecular weight changes over time during ultrasonication of the oxidative decomposition products. Figure 5c,d show the GPC graphs of the products obtained over time for samples 70 and F70, respectively.

For sample 70, in which the alginate monomer units were preserved with selective glycosidic linkage cleavage, the molecular weight was initially 4230 Da and decreased to 3960 Da (after 3 h) and 3410 Da (after 6 h). Finally, after 10 h of reaction, the molecular weight became ~3380 Da (~20.0% decrease). Polydispersity showed similar values of 1.19–1.52, indicating no noticeable changes in the molecular weight distribution after ultrasonication of sample 70. Analysis of molecular weight distribution from the GPC results (Figure 5c) revealed that, as ultrasonication time increased, polymer chains with molecular weights exceeding 2400 Da underwent cleavage, resulting in the predominant formation of low-molecular-weight alginate in the range of 1500–2400 Da. In addition, small amounts of oligomers, ranging from 400 to 1500 Da (dimers to heptamers), were observed. The molecular weight of sample 90 remained at ~2730 Da for up to 6 h of ultrasonication but slightly decreased to 2310 Da after 10 h of reaction. By contrast, no significant changes were observed in samples 110 and 130 after ultrasonication.

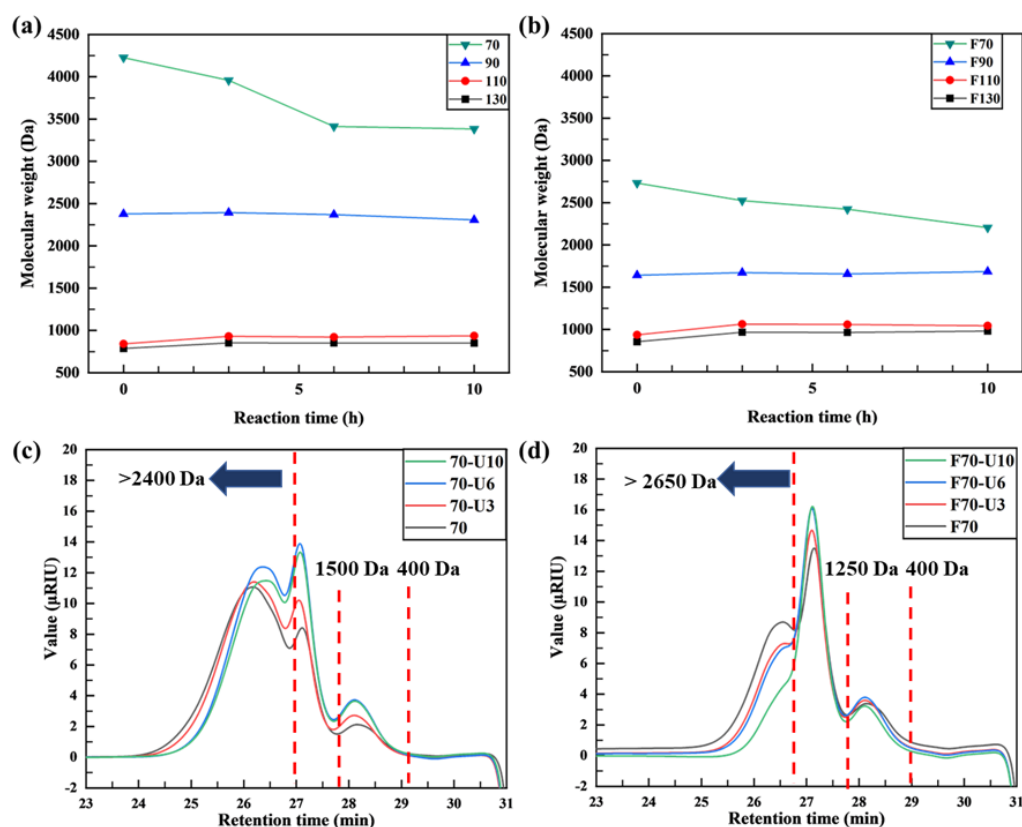


Figure 5. (a,b) Molecular weight of products by ultrasonication time and GPC spectra of (c) 70 and (d) F70 after ultrasonication.

For sample F70, in which the alginate chains were partially randomly cleaved, the initial molecular weight was 2730 Da. During ultrasonication, the molecular weight decreased to 2530 Da after 3 h, 2420 Da after 6 h, and finally to 2210 Da (~19.3% decrease) after 10 h. Polydispersity exhibited similar ranges of 1.26–1.62, indicating no noticeable changes among molecular weight distribution after ultrasonication on sample F70. As the ultrasonication time increased, high-molecular-weight polymers (>2650 Da) were depolymerized to low-molecular-weight alginate in the range of 1250–2650 Da. However, oligomers ranging from 400 to 1250 Da (dimers to hexamers) did not change significantly with increasing ultrasonication time. For samples F90, F110, and F130, it was challenging to observe notable changes in average molecular weight with respect to the ultrasonication time.

Additional FT–IR and NMR analyses were conducted on samples 70 and F70, which exhibited significant molecular weight changes during ultrasonication, to investigate the structural changes.

3.2.2. FT–IR Analysis

FT–IR analysis was conducted to confirm the structural characteristics of the products obtained from the ultrasound treatment of samples 70 and F70 (Figure 6).

First, when investigating the infrared absorption bands of sample 70 as a function of reaction time, it can be observed that the peaks at $947\text{--}951\text{ cm}^{-1}$ are maintained, which correspond to the uronic acid monomers in alginate, as well as the peaks at $1040\text{--}1045$, $1079\text{--}1090$, and $1122\text{--}1125\text{ cm}^{-1}$ attributed to alginate's characteristic infrared absorption wavelengths. However, the peak at 1170 cm^{-1} , corresponding to the glycosidic linkage, gradually decreases as the ultrasonication time increases (Figure 6b). From these results, it can be inferred that the uronic acid structure remained intact, while the glycosidic linkage connecting the monomers was selectively cleaved, indicating selective depolymerization [25–37].

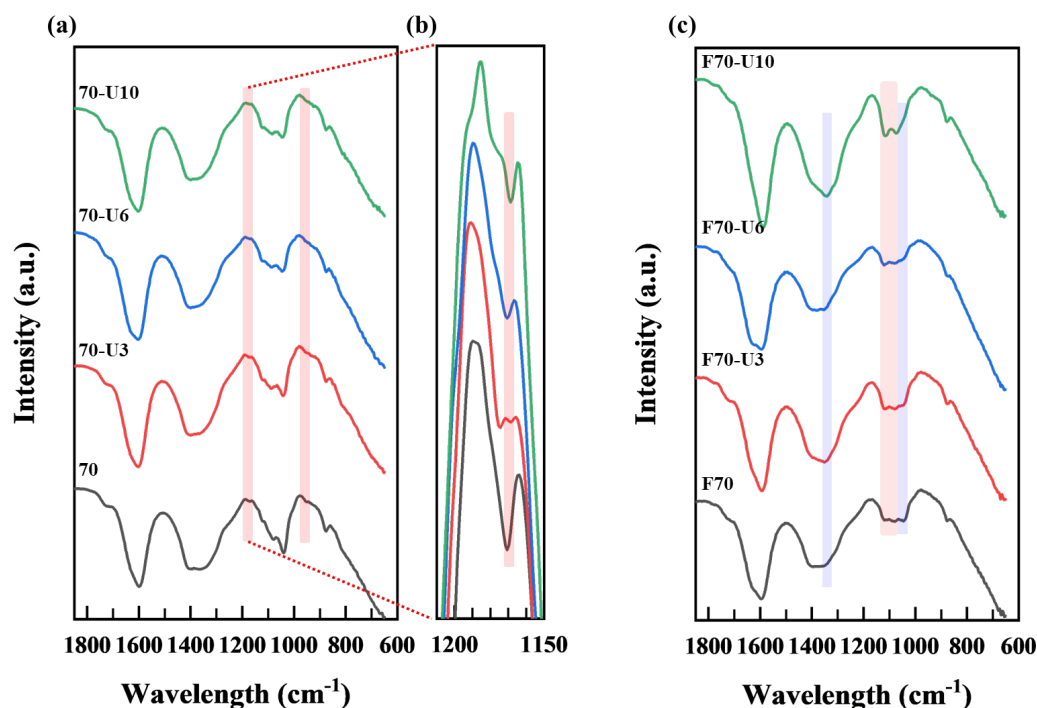


Figure 6. FT–IR spectra of products after ultrasonication with reactant (a) 70, (b) 70 (1150–1200 cm^{-1}), and (c) F70.

Furthermore, for sample F70, as the ultrasonication time increased, the absorption wavelength at 1045 cm^{-1} attributed to C–O stretching vibrations within the monosaccharide ring decreased. Peaks at $1117\text{--}1120$ and $1079\text{--}1080 \text{ cm}^{-1}$, known as the pyranose ring regions, remained unchanged. Conversely, the peak at 1350 cm^{-1} , associated with --CH_3 and $\text{--CH}_2\text{--}$ deformation vibrations, tended to increase. Therefore, it can be deduced that, as the ultrasonication time increased, depolymerization occurred randomly via the cleavage of glycosidic linkages (C–O–C) among the alginate monomer units or pyranose ring opening [25–37]. For the other samples, no significant differences were observed, regardless of ultrasonication time.

3.2.3. NMR Analysis

Figure 7 shows the NMR results of the products obtained from the ultrasonication of samples 70 and F70 as a function of reaction time. When studying the NMR spectra as a function of reaction time for sample 70, it can be observed that the peaks in the 3.5–5.6 ppm region, representing the characteristics of alginate, show an increasing sharpness and intensity trend. In addition, no peaks are observed in the 2.1–2.3 and 8.7–8.8 ppm regions, indicating that no opening of pyranose rings occurred. Therefore, depolymerization during the ultrasonication of sample 70 was inferred to selectively break the glycosidic bonds while preserving the alginate monomer units [11,38–41].

For sample F70, as the ultrasonication time increased, the peaks at 2.1–2.3 ppm (methyl groups, --CH_3 , and carbon chains, $\text{--CH}_2\text{--}$) and 8.7–8.8 ppm (aldehyde, --CHO) increased. From this, it can be inferred that with increasing ultrasonication time for this sample, the opening of pyranose rings, attributed to uronic acid, proceeds, and the polymer chains are randomly cleaved (random scission) [11,38–41].

In summary, when high-frequency ultrasonication was applied to the products of the oxidative decomposition reaction, the following observations were made:

1. For sample 70, ultrasonication led to the selective cleavage of glycosidic bonds within the alginate structure with increasing reaction time. This process generated low-molecular-weight polymers, particularly dimers to heptamers, from high-molecular-weight polymers ($>2400 \text{ Da}$) through a selective depolymerization process.

- Conversely, when sample F70 was subjected to ultrasonication, the alginate was randomly depolymerized by the opening of the pyranose rings within the alginate structure or the cleavage of glycosidic bonds in the monomer chains. Consequently, low-molecular-weight polymers in the range of 1250–2650 Da were generated because of this random depolymerization process.
- In the case of alginate sources other than the aforementioned samples, ultrasonication did not result in further depolymerization. This suggests that the hydroxyl radicals generated by ultrasound primarily target glycosidic bonds that connect the monomer units of the polymer, leading to selective depolymerization and generation of low-molecular-weight species, such as dimers or oligomers.

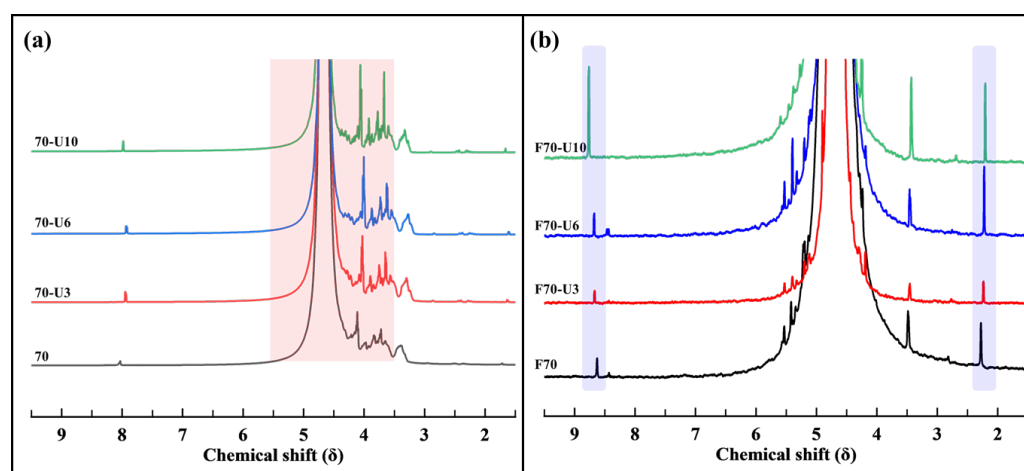


Figure 7. $^1\text{H-NMR}$ spectra of products after ultrasonication with reactant (a) 70 and (b) F70.

These findings indicate that applying high-frequency ultrasonication can induce selective depolymerization in alginate structures, forming low-molecular-weight products with specific outcomes depending on the reaction conditions and initial alginate source.

From the results for oxidative decomposition followed by high-frequency ultrasonication of alginate, we suggest the conceptual depolymerization of alginate in Figure 8.

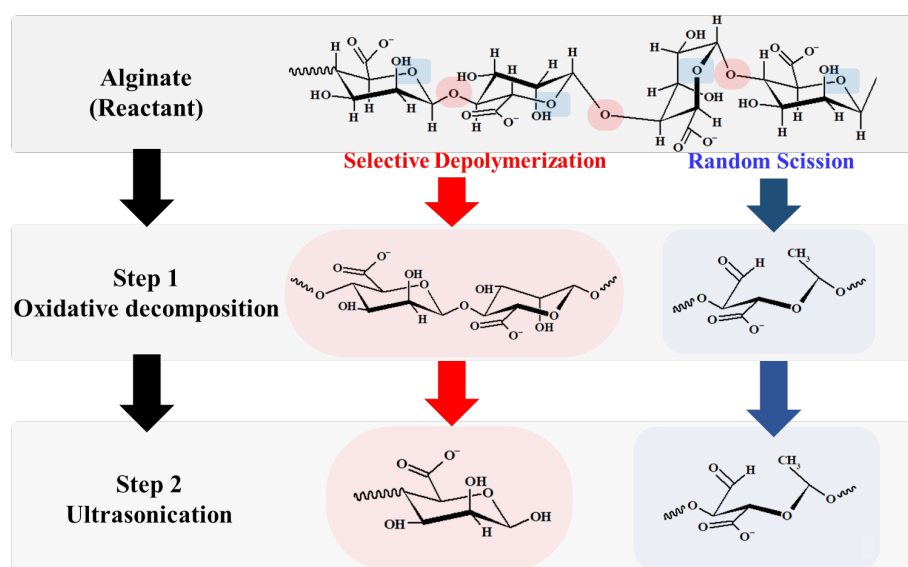


Figure 8. Conceptual depolymerization of alginate via oxidative decomposition (Step 1) and ultrasonication (Step 2).

4. Conclusions

In this study, we conducted a two-step depolymerization reaction involving the oxidative decomposition of alginate, the main component of seaweed biomass, followed by high-frequency ultrasound. Oxidative decomposition resulted in a reduction of over 99% in molecular weight as reaction temperature increased. From a molecular structure perspective, the reaction temperature is a key factor. When alginate was decomposed with H₂O₂ at the reaction temperatures of 70 and 90 °C, alginate units (mannuronic acids and guluronic acids) were preserved and selective depolymerization occurred primarily through the cleavage of glycosidic bonds by hydroxyl radicals. However, all polymer chains were randomly cleaved at reaction temperatures of 110 and 130 °C.

Ultrasonication of the alginates resulted in additional molecular weight decreases in the high-molecular-weight alginate oligomers (>2400 Da). However, different trends were observed depending on whether the alginate monomer unit chains were preserved. When the alginate units remained, the glycosidic bonds between the alginate unit chains were selectively cleaved. However, when the alginate units were cleaved, ultrasound-induced depolymerization led to ring-opening reactions between the alginate chains. This result suggests that alginate depolymerization can be selectively controlled by the depolymerization method, initial alginate structure, and reaction conditions.

Supplementary Materials: The following supporting information can be downloaded at: <https://www.mdpi.com/article/10.3390/cleantechnol5040069/s1>, Table S1: The molecular weight and polydispersity of the products based on oxidation reaction temperature and the use of oxidants; Table S2: Peak assignments for carboxylic anions, aliphatic C-H, glycosidic linkages, pyranose rings, and uronic acid groups; Table S3: The molecular weight for each raw material and products of ultrasonication; Table S4: Polydispersity for each raw material and products of ultrasonication; Figure S1: GPC spectra for raw alginate material and products after oxidative decomposition with (a) H₂O₂ (70–130) and (b) H₂O₂ + Fe₃O₄ (F70–F130).

Author Contributions: Conceptualization, H.C.W.; validation, Y.H.S.; investigation, Y.H.S.; writing—original draft preparation, Y.H.S.; writing—review and editing, Y.H.S., H.C.W. and J.L.; supervision, H.C.W. and J.L.; project administration, J.L.; funding acquisition, J.L. All authors have read and agreed to the published version of the manuscript.

Funding: This research was supported by the National Research Foundation (NRF) [2022R1F1A1076522] and Korea Institute of Marine Science and Technology Promotion (KIMST) funded by the Ministry of Oceans and Fisheries, Republic of Korea (20220258).

Institutional Review Board Statement: Not applicable.

Informed Consent Statement: Not applicable.

Data Availability Statement: Data are contained within the article and Supplementary Materials.

Conflicts of Interest: The authors declare no conflict of interest.

References

1. Song, M.; Pham, H.D.; Seon, J.; Woo, H.C. Marine brown algae: A conundrum answer for sustainable biofuels production. *Renew. Sustain. Energy Rev.* **2015**, *50*, 782–792. [[CrossRef](#)]
2. Luo, L.; van der Voet, E.; Huppes, G. Biorefining of lignocellulosic feedstock—Technical, economic and environmental considerations. *Bioresour. Technol.* **2010**, *101*, 5023–5032. [[CrossRef](#)] [[PubMed](#)]
3. Draget, K.I.; Skjåk-Bræk, G.; Smidsrød, O. Alginate based new materials. *Int. J. Biol. Macromol.* **1997**, *21*, 47–55. [[CrossRef](#)] [[PubMed](#)]
4. Zia, K.M.; Zia, F.; Zuber, M.; Rehman, S.; Ahmad, M.N. Alginate based polyurethanes: A review of recent advances and perspective. *Int. J. Biol. Macromol.* **2015**, *79*, 377–387. [[CrossRef](#)] [[PubMed](#)]
5. Jeon, W.; Ban, C.; Park, G.; Yu, T.-K.; Suh, J.-Y.; Woo, H.C.; Kim, D.H. Catalytic hydrothermal conversion of macroalgae-derived alginate: Effect of pH on production of furfural and valuable organic acids under subcritical water conditions. *J. Mol. Catal. A Chem.* **2015**, *399*, 106–113. [[CrossRef](#)]
6. Jeon, W.; Ban, C.; Park, G.; Kim, J.E.; Woo, H.C.; Kim, D.H. Catalytic conversion of macroalgae-derived alginate to useful chemicals. *Catal. Surv. Asia* **2016**, *20*, 195–209. [[CrossRef](#)]

7. Koyanagi, S.; Tanigawa, N.; Nakagawa, H.; Soeda, S.; Shimeno, H. Oversulfation of fucoidan enhances its anti-angiogenic and antitumor activities. *Biochem. Pharmacol.* **2003**, *65*, 173–179. [[CrossRef](#)] [[PubMed](#)]
8. Schaeffer, D.J.; Krylov, V.S. Anti-HIV activity of extracts and compounds from algae and cyanobacteria. *Ecotoxicol. Environ. Saf.* **2000**, *45*, 208–227. [[CrossRef](#)]
9. Zhang, C.; Li, M.; Rauf, A.; Khalil, A.A.; Shan, Z.; Chen, C.; Rengasamy, K.R.; Wan, C. Process and applications of alginate oligosaccharides with emphasis on health beneficial perspectives. *Crit. Rev. Food Sci. Nutr.* **2023**, *63*, 303–329. [[CrossRef](#)]
10. Wang, M.; Chen, L.; Zhang, Z. Potential applications of alginate oligosaccharides for biomedicine—A mini review. *Carbohydr. Polym.* **2021**, *271*, 118408. [[CrossRef](#)]
11. Choi, S.K.; Choi, Y.S. Depolymerization of alginates by hydrogen peroxide/ultrasonic irradiation. *Polymers* **2011**, *35*, 444–450.
12. Tecson, M.G.; Abad, L.V.; Ebajo, V.D., Jr.; Camacho, D.H. Ultrasound-assisted depolymerization of kappa-carrageenan and characterization of degradation product. *Ultrason. Sonochem.* **2021**, *73*, 105540. [[CrossRef](#)] [[PubMed](#)]
13. Bouanati, T.; Colson, E.; Moins, S.; Cabrera, J.-C.; Eeckhaut, I.; Raquez, J.-M.; Gerbaux, P. Microwave-assisted depolymerization of carrageenans from *Kappaphycus alvarezii* and *Euचेuma spinosum*: Controlled and green production of oligosaccharides from the algae biomass. *Algal Res.* **2020**, *51*, 102054. [[CrossRef](#)]
14. Holme, H.K.; Lindmo, K.; Kristiansen, A.; Smidsrød, O. Thermal depolymerization of alginate in the solid state. *Carbohydr. Polym.* **2003**, *54*, 431–438. [[CrossRef](#)]
15. Haouache, S.; Karam, A.; Chave, T.; Clarhaut, J.; Amaniampong, P.N.; Fernandez, J.M.G.; Vigier, K.D.O.; Capron, I.; Jérôme, F. Selective radical depolymerization of cellulose to glucose induced by high frequency ultrasound. *Chem. Sci.* **2020**, *11*, 2664–2669. [[CrossRef](#)]
16. Wong, T.Y.; Preston, L.A.; Schiller, N.L. Alginate lyase: Review of major sources and enzyme characteristics, structure–function analysis, biological roles, and applications. *Annu. Rev. Microbiol.* **2000**, *54*, 289–340. [[CrossRef](#)]
17. Yamasaki, M.; Ogura, K.; Hashimoto, W.; Mikami, B.; Murata, K. A structural basis for depolymerization of alginate by polysaccharide lyase family-7. *J. Mol. Biol.* **2005**, *352*, 11–21. [[CrossRef](#)] [[PubMed](#)]
18. Burana-Osot, J.; Hosoyama, S.; Nagamoto, Y.; Suzuki, S.; Linhardt, R.J.; Toida, T. Photolytic depolymerization of alginate. *Carbohydr. Res.* **2009**, *344*, 2023–2027. [[CrossRef](#)]
19. Soukaina, B.; Zainab, E.A.-T.; Guillaume, P.; Halima, R.; Philippe, M.; Cherkaoui, E.M.; Cédric, D. Radical depolymerization of alginate extracted from Moroccan brown seaweed *Bifurcaria bifurcata*. *Appl. Sci.* **2020**, *10*, 4166. [[CrossRef](#)]
20. Haber, F.; Weiss, J. The catalytic decomposition of hydrogen peroxide by iron salts. *Proc. R. Soc. London Ser. A Math. Phys. Sci.* **1934**, *147*, 332–351.
21. Jérôme, F.; Chatel, G.; Vigier, K.D.O. Depolymerization of cellulose to processable glucans by non-thermal technologies. *Green Chem.* **2016**, *18*, 3903–3913. [[CrossRef](#)]
22. McKenzie, T.G.; Karimi, F.; Ashokkumar, M.; Qiao, G.G. Ultrasound and sonochemistry for radical polymerization: Sound synthesis. *Chem. Eur. J.* **2019**, *25*, 5372–5388. [[CrossRef](#)] [[PubMed](#)]
23. Roy, K.; Moholkar, V.S. *p*-nitrophenol degradation by hybrid advanced oxidation process of heterogeneous Fenton assisted hydrodynamic cavitation: Discernment of synergistic interactions and chemical mechanism. *Chemosphere* **2020**, *283*, 131114. [[CrossRef](#)] [[PubMed](#)]
24. Ahn, H.J.; Kang, K.S.; Song, Y.H.; Lee, D.H.; Kim, M.H.; Lee, J.; Woo, H.C. Effect of cardanol content on the antibacterial films derived from alginate-PVA blended matrix. *Clean Technol.* **2022**, *28*, 24–31.
25. Huang, R.; Pal, R.; Moon, G. Characteristics of sodium alginate membranes for the pervaporation dehydration of ethanol–water and isopropanol–water mixtures. *J. Membr. Sci.* **1999**, *160*, 101–113. [[CrossRef](#)]
26. Zain, N.A.M.; Suhaimi, M.S.; Idris, A. Development and modification of PVA–alginate as a suitable immobilization matrix. *Process Biochem.* **2011**, *46*, 2122–2129. [[CrossRef](#)]
27. Fertah, M.; Belfkira, A.; Taourirte, M.; Brouillette, F. Extraction and characterization of sodium alginate from Moroccan *Laminaria digitata* brown seaweed. *Arab. J. Chem.* **2017**, *10*, S3707–S3714. [[CrossRef](#)]
28. González-López, N.; Moure, A.; Domínguez, H. Hydrothermal fractionation of *Sargassum muticum* biomass. *J. Appl. Phycol.* **2012**, *24*, 1569–1578. [[CrossRef](#)]
29. Margenot, A.J.; Calderón, F.J.; Parikh, S.J. Limitations and potential of spectral subtractions in Fourier-transform infrared spectroscopy of soil samples. *Soil Sci. Soc. Am. J.* **2016**, *80*, 10–26. [[CrossRef](#)]
30. Anjali, T. Modification of carboxymethyl cellulose through oxidation. *Carbohydr. Polym.* **2012**, *87*, 457–460. [[CrossRef](#)]
31. Vijayakumar, S.; Malaikozhundan, B.; Parthasarathy, A.; Saravanakumar, K.; Wang, M.-H.; Vaseeharan, B. Nano biomedical potential of biopolymer chitosan-capped silver nanoparticles with special reference to antibacterial, antibiofilm, anticoagulant and wound dressing material. *J. Clust. Sci.* **2020**, *31*, 355–366. [[CrossRef](#)]
32. Singh, K.; Devi, S.; Bajaj, H.; Ingole, P.; Choudhari, J.; Bhrambhatt, H. Optical resolution of racemic mixtures of amino acids through nanofiltration membrane process. *Sep. Sci. Technol.* **2014**, *49*, 2630–2641. [[CrossRef](#)]
33. Caykara, T.; Demirci, S. Preparation and characterization of blend films of poly (vinyl alcohol) and sodium alginate. *J. Macromol. Sci. Part A* **2006**, *43*, 1113–1121. [[CrossRef](#)]
34. El Nembr, A.; Eleryan, A.; Mashaly, M.; Khaled, A. Rapid synthesis of cellulose propionate and its conversion to cellulose nitrate propionate. *Polym. Bull.* **2021**, *78*, 4149–4182. [[CrossRef](#)]

35. Sakugawa, K.; Ikeda, A.; Takemura, A.; Ono, H. Simplified method for estimation of composition of alginates by FTIR. *J. Appl. Polym. Sci.* **2004**, *93*, 1372–1377. [[CrossRef](#)]
36. Margariti, C. The application of FTIR microspectroscopy in a non-invasive and non-destructive way to the study and conservation of mineralised excavated textiles. *Herit. Sci.* **2019**, *7*, 63. [[CrossRef](#)]
37. Cardenas-Jiron, G.; Leal, D.; Matsuhiro, B.; Osorio-Roman, I. Vibrational spectroscopy and density functional theory calculations of poly-D-mannuronate and heteropolymeric fractions from sodium alginate. *J. Raman Spectrosc.* **2011**, *42*, 870–878. [[CrossRef](#)]
38. Huamani-Palomino, R.G.; Córdova, B.M.; Pichilingue, L.E.R.; Venâncio, T.; Valderrama, A.C. Functionalization of an alginate-based material by oxidation and reductive amination. *Polymers* **2021**, *13*, 255. [[CrossRef](#)] [[PubMed](#)]
39. Gomez, C.G.; Rinaudo, M.; Villar, M.A. Oxidation of sodium alginate and characterization of the oxidized derivatives. *Carbohydr. Polym.* **2007**, *67*, 296–304. [[CrossRef](#)]
40. Delattre, C.; Michaud, P.; Elboutachfaiti, R.; Courtois, B.; Courtois, J. Production of oligocellouronates by biodegradation of oxidized cellulose. *Cellulose* **2006**, *13*, 63–71. [[CrossRef](#)]
41. Luo, P.; Liu, L.; Xu, W.; Fan, L.; Nie, M. Preparation and characterization of aminated hyaluronic acid/oxidized hydroxyethyl cellulose hydrogel. *Carbohydr. Polym.* **2018**, *199*, 170–177. [[CrossRef](#)] [[PubMed](#)]

Disclaimer/Publisher’s Note: The statements, opinions and data contained in all publications are solely those of the individual author(s) and contributor(s) and not of MDPI and/or the editor(s). MDPI and/or the editor(s) disclaim responsibility for any injury to people or property resulting from any ideas, methods, instructions or products referred to in the content.